International Journal of Molecular Sciences

MDPI

Article

Effect of Cyclic Stretch on Vascular Endothelial Cells and Abdominal Aortic Aneurysm (AAA): Role in the Inflammatory Response.

Martina Ramella[1], Giulia Bertozzi[1], Luca Fusaro[1,2], Maria Talmon[1], Marcello Manfredi[3,5], Marta Calvo Catoria[1,2], Francesco Casella[4], Carla M. Porta[4], Renzo Boldorini[1], Luigia G. Fresu[1], Emilio Marengo[5], Francesca Boccafoschi[1,2]*

[1] Department of Health Science, University of Piemonte Orientale (UPO), via Solaroli 17, Novara, Italy.
[2] TissueGraft s.r.l. Spin-off of University of Piemonte Orientale (UPO), via Canobio 4/6, Novara, Italy.
[3] ISALIT s.r.l. Spin-off of DISIT, University of Piemonte Orientale (UPO), Alessandria, Italy,
[4] Vascular Surgery Unit, Ospedale Maggiore della Carità, Novara, Italy.
[5] Department of Sciences and Technological Innovation, University of Piemonte Orientale (UPO), Alessandria, Italy,
* Correspondence: Prof. Francesca Boccafoschi, via Solaroli 17, 28100 Novara, Italy. E-mail: francesca.boccafoschi@med.uniupo.it; telephone number +39 0321-660556.

Received: date; Accepted: date; Published: date

Abstract: Abdominal aortic aneurysm (AAA) is a focal dilatation of the aorta, caused by both genetic and environmental factors. Although vascular endothelium plays a key role in AAA progression, the biological mechanisms underlying the mechanical stress involvement are only partially understood. In this study, we developed an *in vitro* model to characterize the role of mechanical stress as a potential trigger of endothelial deregulation in terms of inflammatory response bridging between endothelial cells (ECs), inflammatory cells, and matrix remodeling. In AAA patients, data revealed different degrees of calcification, inversely correlated with wall stretching and also with inflammation and extracellular matrix degradation. In order to study the role of mechanical stimulation, endothelial cell line (EA.hy926) has been cultured in healthy (10% strain) and pathological (5% strain) dynamic conditions using a bioreactor. In presence of TNF-α, high levels of MMP-9 expression and inflammation are obtained, while mechanical stimulation significantly counteracts the TNF-α effects. Moreover, physiological deformation also plays a significant role in the control of the oxidative stress. Overall our findings indicate that, due to wall calcification, in AAA there is a significant change in terms of decreased wall stretching.

Keywords: cardiovascular diseases; abdominal aortic aneurysm; oxidative stress; inflammation; calcification; cyclic stretch

1. Introduction

Abdominal aortic aneurysm (AAA) is a degenerative disease caused by permanent dilatation of the aorta in the abdominal infrarenal tract. [1] AAA annual incidence is 0.4%-0.67% in western population [2–4], while the prevalence is 4%-8% [5–7], and it is more common in men than in women. Although the exact aetiology of AAA is unknown, there are several risk factors related to AAA development such as male gender, age (≥ 50 years old), smoking habits, atherosclerosis and hypertension, and some genetic factors. [8,9] Aneurysm can develop slowly, even silently and asymptomatically until the rupture occurs, causing massive haemorrhage with an elevated risk of death due to hypovolemic and haemorrhagic shock. [10] Extracellular matrix (ECM) degradation and oxidative stress represent hallmarks of AAA progression. [11] Calcification is commonly found

within the aneurysm wall and leading to wall stiffening, and eventually to its rupture. [12] Moreover, increased mechanical stresses due to turbulent flow within the wall contribute to AAA progression and rupture. [13] The ability of a vascular wall to relax and passively contract depending on pressure changes and blood flow is a physiological characteristic of large elastic arteries, and it is defined as "compliance". Bloodstream in the vascular compartment follows the laws of laminar flow; laminar flow is altered by the reduction of flow velocity (blood stasis) as well as by the fluctuation of flow (turbulence). The classical turbulent flow causes endothelial damage as it leads to the generation of flows that are contrary to the direction of the circulatory current, also generating pockets of stasis. [14] In arterial aneurysms, especially those with saccular morphology, there may be a slowing down of flow until blood stasis.

Blood flow in the arterial aneurysm follows La Place's law, which explains how the parietal tension (T) depends on the transmural pressure (Ptm), the wall thickness (d) and the radius of the container (r) according to the equation:

$$T = (Ptm * r)/d.$$

If the volume increases, the parietal voltage increases. In fact, if the vessel expands, the increase in the radius coupled with the decrease in the wall thickness increases the tension required to counteract the transmural pressure. Blood vessels function as viscoelastic tubes and respond to a transmural pressure gradient as a function of blood vessel wall composition. As vessel wall is subjected to a transmural pressure gradient, a portion of the intraluminal energy is used to stretch the fibers within the wall. The energy stored within the blood vessel fibers is later released back into the system, upon closure of the aortic valve. As intraluminal pressure oscillates, the constant loading and unloading of the fibers in the vessel wall result in a change in diameter of the blood vessel, which is noted clinically as a palpable pulse. Although vascular ECs and vascular smooth muscle cells (vSMCs) are exposed to both types of mechanical forces, shear stress resulting from blood flow is sensed mainly by ECs [15], whereas both ECs and vSMCs are subjected to cyclic stretch resulting from pulsatile pressure. In pathological remodeling, ECs can be influenced on structural as well as functional aspects. Firstly, they can change morphology, acquiring a bigger size and an irregular shape; they can also lose most of their regulatory roles. Endothelial layer can become more permeable, allowing the transit of several substances and vSMC infiltration. Endothelium shows inflammatory features, and it is characterized by the hyperexpression of proinflammatory cytokines (IL-1, IL-6, TNF-α), proinflammatory chemokines (IL-8, MCP-1, and regulated upon activation, normal T-Cell expressed- and secreted- RANTES) [16,17] and cell adhesion molecules (CAMs) such as selectins and integrins, [18] with a significant production of reactive oxygen species (ROS), in particular hydrogen peroxide (H_2O_2), superoxide (O_2^-), and hydroxyl radical (.OH). [19,20] Deregulation of NADPH oxidase (NOX), xanthine oxidase (XO), superoxide dismutase (SOD), thioredoxin (TRX), and catalase results in extreme ROS production. [21,22] Moreover, ROS regulate ECM remodeling, acting directly on matrix metalloproteinases (MMPs) up-regulation, activating nuclear factor kB (NF-kB) and activator protein (AP-1). [23–25] The aim of this work is to clarify the role of vascular wall stretching in the maintenance of vascular physiology reproducing *in vitro* the pathological dilatation (static and 5%), due to calcification, and physiological (10%) cyclic (1 Hz) stretch of the vessel wall, in order to study the effects of mechanical stress on ECs functionality in terms of inflammation, matrix remodeling, and oxidative stress production.

2. Results

2.1. Relationship between wall stress and degree of calcification

Patient-specific AAA geometries are reconstructed, and structural analysis is performed to calculate the wall stresses of the AAA models and their calcification. In figure 1A is shown how the wall dilatation changes in relation to the amount of calcification. Retrospective analyses of literature show that the aortic dilatation in healthy donors is 10% considering the ratio between systole and diastole; this data is confirmed also by our measures on healthy controls. In fact, in presence of

aneurysm the dilatation is less than 10%, and it decreases when the calcification index increase (Figure 1A). Control aortas and AAA sections are stained with Von Kossa to confirm the calcification degrees obtained by the measurements with computed axial tomography (CAT) analysis. As expected, controls do not show any calcium accumulation, while AAA tissues present dark spots (calcium deposition) in particular in the medial layer, in a directly proportional manner to the degree of calcification, as shown by related quantification (Figure 1B and 1C).

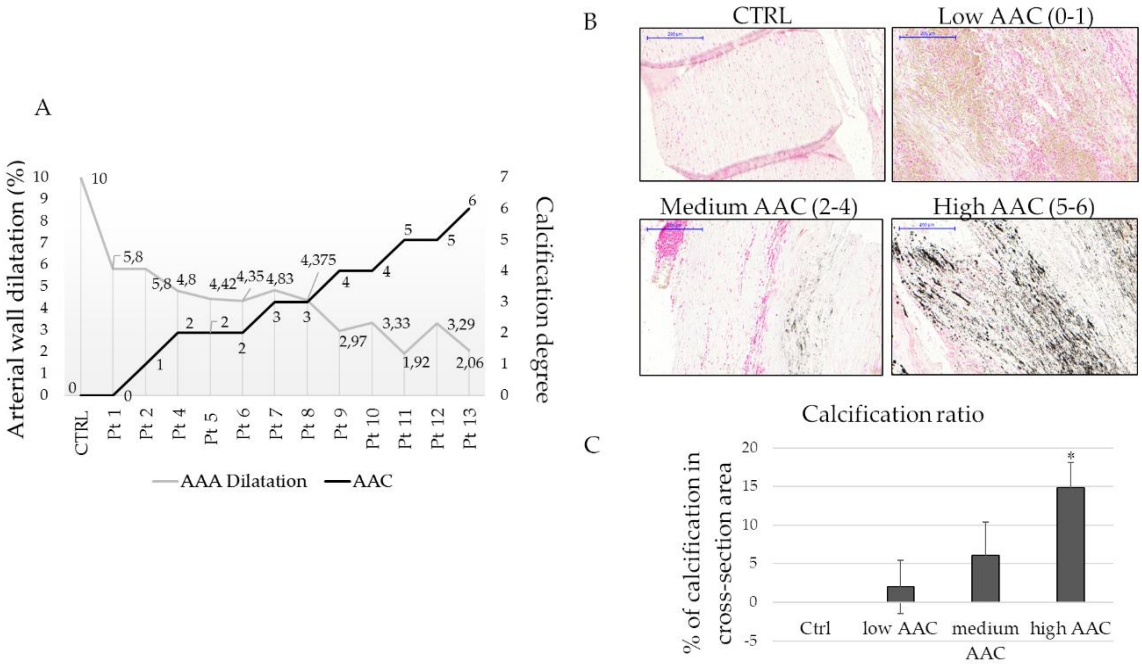

Figure 1. Wall stress and calcification correlation, (**a**) Graph showing the relation between AAA dilatation and calcification (AAC, aortic aneurysm calcification); (**b**) Representative images of calcification degree evaluated by Von Kossa staining in paraffin-embedded tissues. Scale bar 200 μm; (**c**) Quantification of calcium content in healthy tissues (CTRL) and aneurysm tissues evaluated by ImageJ software. * indicates $p \leq 0.05$ respect to control.

2.2. Correlation between calcium deposition and inflammation

Knowing that AAA is characterized by an inflammatory condition, different inflammatory markers related to inflammatory cells are investigated, in particular CD4, CD20, and CD68, respectively for T-helper lymphocyte, B-cell, and macrophage identification. Control tissues are negative for all the markers, while in the low and medium AAC index all these markers are significantly represented. High AAC index tissues show a decrease of the inflammatory population correlated to CD4, CD20, and CD68 markers with respect to low and medium indexes. (Figure 2).

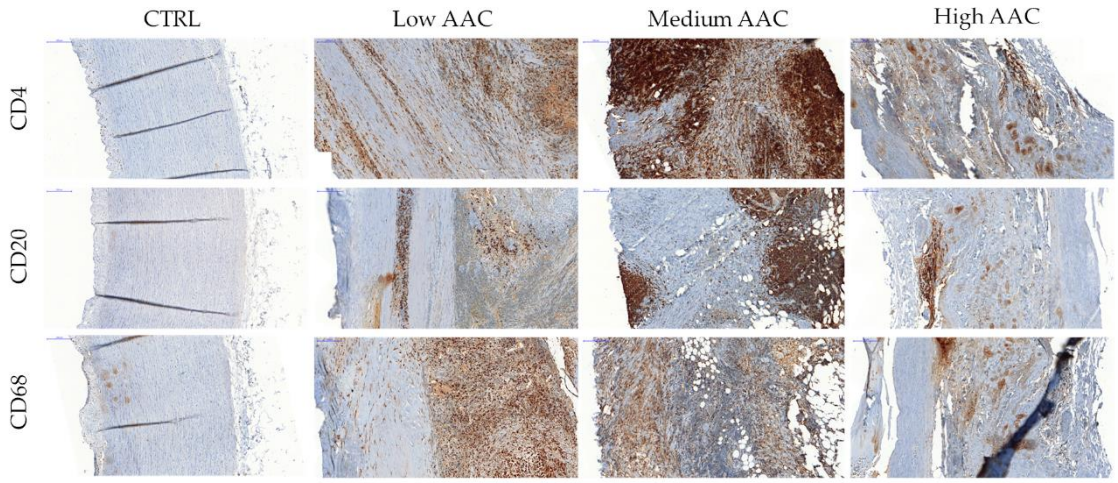

Figure 2. Inflammatory cell infiltration in AAA. Representative immunohistochemistry for anti CD4, CD8, CD68 staining. CD4+ is performed for T-helper lymphocytes, CD8+ for T-killer, and CD68 for monocytes-macrophage. Healthy aorta, represented on the left, is negative for inflammatory cells infiltration. Scale bar 200 μm.

Other pro-inflammatory and calcification markers were investigated on tissue lysate, such as MMP-9, IL-6 and osteopontin (Figure 3A and 3B). For all the considered markers, we obtain a significant difference between patients and controls. Differences related to the degree of calcification are appreciable: considering MMP-9, samples with medium index of calcification reach the higher expression as observed by western blot assay as well as the higher proteolytic activity, as indicated by zymography assay. The high calcification index indicates also the terminal phase of the degradation, thus MMP-9 results decreased in terms of protein expression and proteolytic activity. Considering IL-6 as an inflammatory marker, it decreases with the progression of calcium accumulation confirming the previous data, particularly, it has the same trend as MMP-9. As expected, patients with high calcification index have an increased expression of OPN, which has an osteogenic activity (Figure 3B). No significant differences are observed between healthy donors and patients in all AAC indices for MMP-2 activity (Figure 3A)

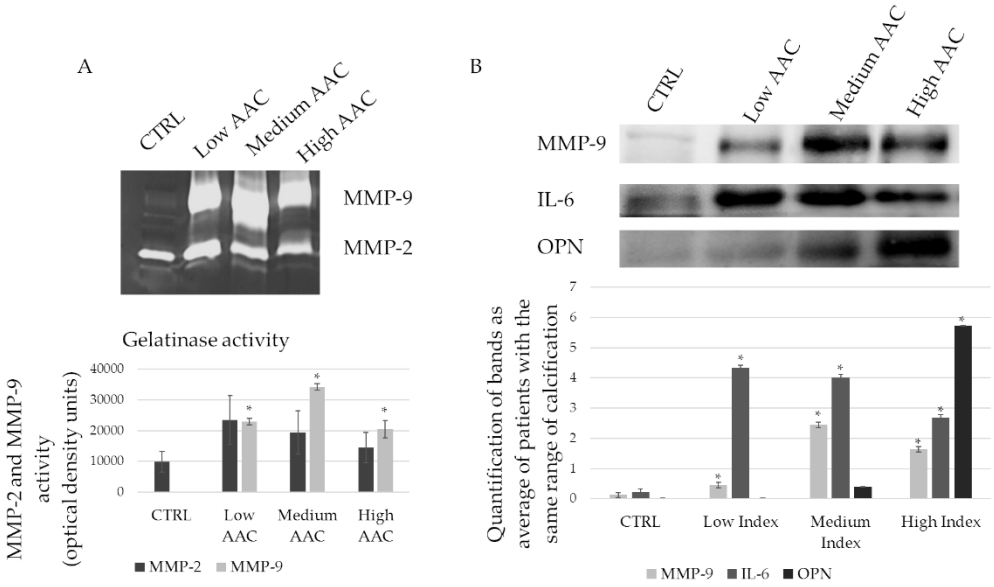

Figure 3. Matrix remodeling, inflammation and calcification in AAA tissues. (**a**) Gelatin zymography performed on tissue lysates of patients with different degree of calcification and the respective quantification of MMP-2 and MMP-9 activity; (**b**) Immunoblot on MMP-9, Il-6, and Osteopontin (OPN) on tissue lysates of patients with different degree of calcification. The graph shows the relative quantification. * statistically significant with respect to control p<0,05.

2.3. Oxidative stress proteins are overexpressed in AAA

The proteomic analysis of aortic abdominal aneurysms and control healthy vessel tissues was performed with LC-MS in order to investigate the modulation of some proteins related to the oxidative stress processes. Table 1 reports the identities, the modulation and the biological functions of seven proteins resulted over expressed in the AAA respect with the healthy tissues. The enrichment of all these proteins indicates that the oxidative stress pathway is strongly involved in the AAA disease and that is particularly upregulated in the aortic abdominal vessel tissue.

Catalase (CATA) and Superoxide dismutase [Mn], mitochondrial (SODM) presented a fold change of 2.51 and 6.95 respectively: these two proteins are involved in the cellular response to oxidative stress pathway, as a result of the exposure to high levels of reactive oxygen species. SODM is also involved in the removal of superoxide radicals and in oxidation-reduction processes. Regarding the last biological function, we found that Protein disulfide-isomerase (PDIA1), Isoform H14 of Myeloperoxidase (PERM), Ceruloplasmin (CERU), Ferritin heavy chain (FRIH), and Ferritin light chain (FRIL) were all strongly upregulted (fold chnge of 2.50, 3.04, 12.83, 21.83 and 26.43) in the AAA tissue.

Table 1. Proteomic analyses results.

PROTEIN	ACCESSION NAME	FOLD CHANGE (p-value < 0.05) AAA/Healthy	BIOLOGICAL FUNCTION
Protein disulfide-isomerase	PDIA1_HUMAN	2,50	oxidation-reduction process
Isoform H14 of Myeloperoxidase	PERM_HUMAN	3,04	oxidation-reduction process
Superoxide dismutase [Mn], mitochondrial	SODM_HUMAN	6,95	cell response to oxidative stress, oxidation-reduction process, removal of superoxide radicals
Ceruloplasmin	CERU_HUMAN	12,83	oxidation-reduction process
Ferritin heavy chain	FRIH_HUMAN	21,83	oxidation-reduction process
Ferritin light chain	FRIL_HUMAN	26,43	oxidation-reduction process
Catalase	CATA_HUMAN	2,51	cell response to oxidative stress

Table 1. Upregulated proteins in AAA vessel tissue after comparison to healthy tissues by proteomic analysis. The upregulated proteins were selected using p value < 0.05.

A protein-protein interaction analysis (Figure 4) of oxidative stress-related proteins was performed using STRING. The network analysis showed a high-connected network among these proteins. Ferritin light chain and Ferritin heavy chain are co-expressed, showed evidence in experimental and association in curated database. Also Superoxide dismutase, Catalase and Protein disulfide-isomerase showed the same connections. The other linked proteins mainly showed text-mining evidence.

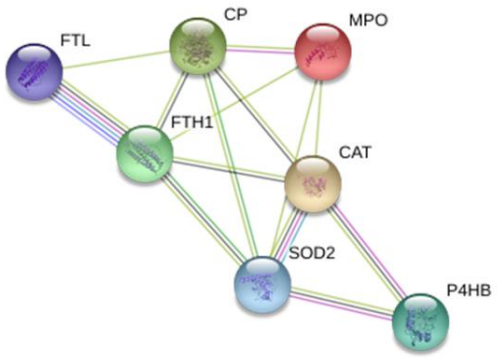

Figure 4. STRING network analysis of oxidative stress-related proteins that are over expressed in AAA vessel tissue respect with normal tissue. A proteome interactomic map was performed using the STRING tool for obtaining cross correlation information. Homo sapiens was selected as a reference organism. Different colored lines represent the existence of different types of evidence. A yellow line indicates text-mining evidence; a purple line, experimental evidence, a cyan line indicates association in curated database and black lines indicates co-expression data.

2.3. Mechanical stimulation drives ROS/Superoxide production in EA.hy926

Since mechanical stimulation seems to play a key role in driving the inflammatory response and matrix remodeling, an *in vitro* dynamic model with physiological and pathological strain parameters, culturing an endothelial cell line (EA.hy 926), was used. The effect of mechanical stimulation (5-10% deformation, 1 Hz frequency) is evaluated in the presence and the absence of an inflammatory stimulus (TNF-α 50 ng/ml) after three days of culture. Figure 5A shows cell morphology when 5% and 10% mechanical strain is applied for 3 days. While no differences were detected in terms of cell viability among the samples, 10% strain cultured cells display an elongated and oriented shape in the

strain direction, whereas random orientation is observed in the other samples (static and 5% strain). In terms of ROS/RNS production, the difference between 10% strained cells (physiological) and 5% strained or static cells (pathological) is confirmed, with lower ROS/RNS production in physiological conditions (Figure 5B and 5C).

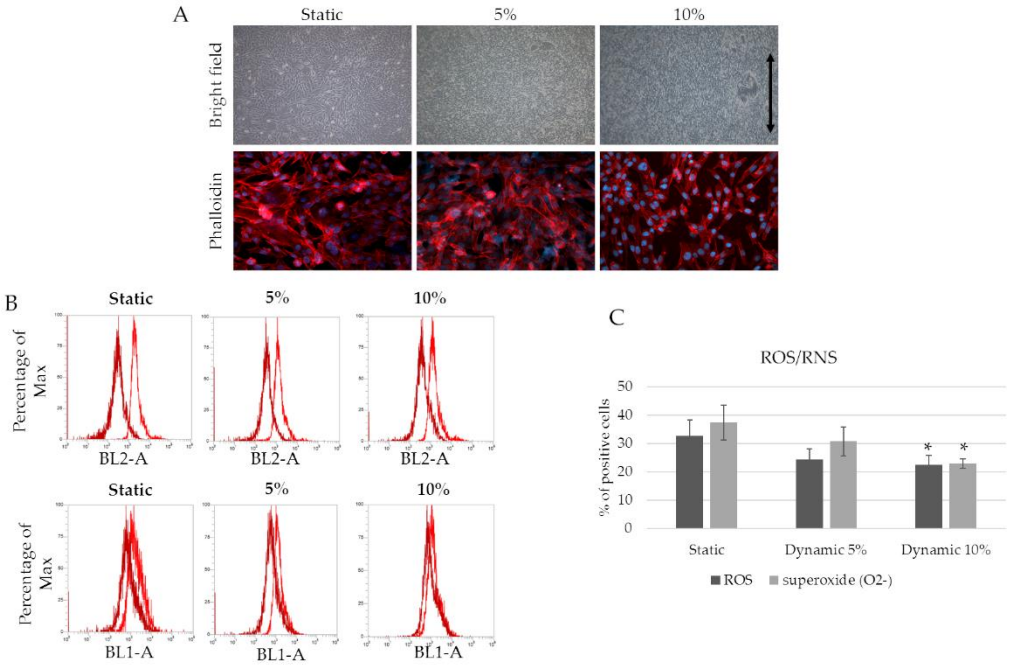

Figure 5. Mechanical strain drives ROS/RNS production. (**a**) EA.hy926 after 3 days of 5% and 10% strain. Phalloidin was used to observe cell morphology; (**b**) FACS analyses for ROS and RNS production. Dark red represents unstained cells, while light red represents the experimental samples. BL2-A for superoxide detection; BL1-A for ROS detection. (**c**) graph of ROS/RNS production * statistically significant with respect to static samples. p<0,05.

2.4. Strain affects CD62E expression and monocytes adhesion

As leukocytes adhesion on endothelium is promoted by CD62E expression on ECs membrane, we evaluated the effect of mechanical stress on CD62E as well (Figure 6A). As expected, E-selectin is upregulated in presence of TNF-α. Data show that the substrate deformation, both 5% and 10% stretching at 1Hz, significantly and proportionally counteracts TNF-α effects on CD62E expression (Figure 6A). In addition, data concerning monocytes adhesion nicely confirm these data. In fact, as shown in Figure 6B, the mechanical deformation, at both 5% and 10% at 1Hz, significantly inhibits the monocytes' adhesion, also in presence of TNF-α.

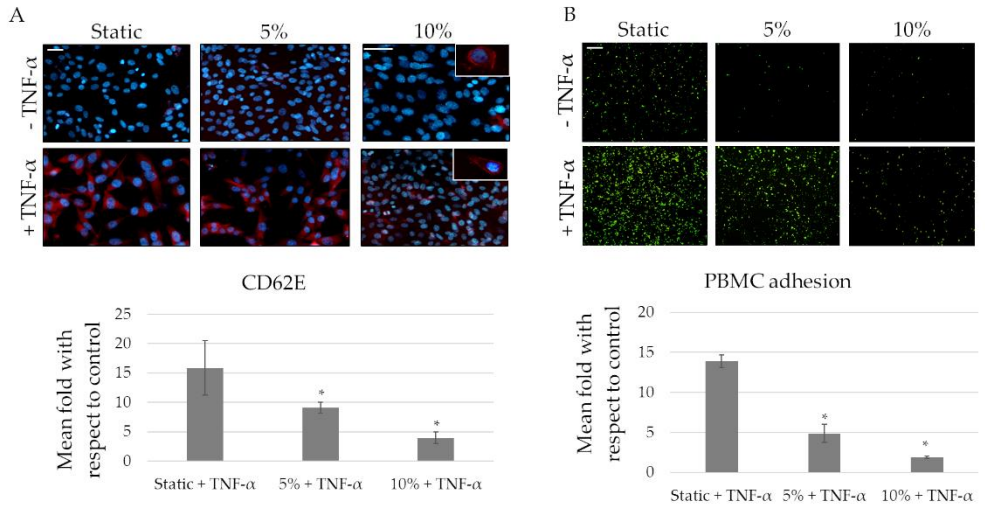

Figure 6. Strain affect inflammation mediated by ECs (**a**) Representative immunofluorescence staining for CD62E after mechanical (5 and 10%) and chemical (TNF-α 50ng/mL) stimulation. CD62E is observed in red while DAPI is used for nuclear staining. Quantification of positive cells expressing CD62E. Normalization of samples stimulated by TNF-α in relation to the respective control. Scale Bar 30 μm * $p \leq 0.05$; (**b**) PBMCs adhesion on endothelial cells. PBMCs are observed in green. Normalization of samples stimulated by TNF-α in relation to the respective control (static, 5% and 10%). Scale Bar 25 μm * $p \leq 0.05$.

2.5. Strain affects MMP-9 expression and activity in ECs.

In static conditions, MMP-9 expression results strongly upregulated in presence of TNF-α. Applying a 5% substrate deformation, no significant inhibition of TNF-α effects is shown, resulting in an unmodified MMP-9 modulation (Figure 7), while no differences are found in absence of TNF-α with respect to static conditions. When a 10% substrate deformation is applied, MMP-9 expression results significantly downregulated in all conditions both in the absence and in the presence of TNF-α.

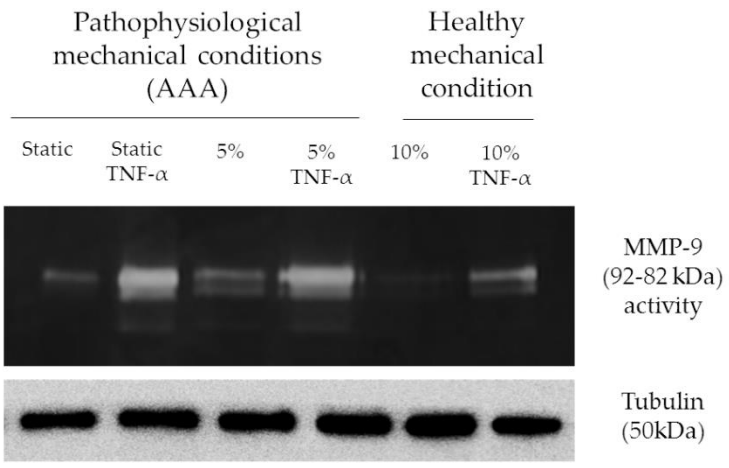

Figure 7. Strain affect MMP-9 expression and activity (a) Representative zymography assay to detect MMP-9 activity and expression after mechanical (5 and 10%) and chemical (TNF-α 50ng/mL) stimulation. Tubulin is used for loading control.

3. Discussion

AAA is characterized by dramatic modifications of the medial layer, and it displays altered mechanical behavior, inflammatory response, and matrix remodeling in the aortic wall. [26] The calcification process has been acknowledged as a degenerative factor in inflammatory arterial diseases. Calcium deposits show a reverse correlation with aortic dilatation and inflammatory cell recruitment, as observed in our clinical data (results summarized in table 2). However, the specific role of aortic dilatation in AAA progression is not completely elucidated. Taking together the results on AAA patients, it is evident that the decrease in dilatation is related to the presence of vascular calcifications in the medial layer. Moreover, the presence of calcification affects MMP-9-promoted matrix remodeling. The severity of calcium deposition influences also IL-6-promoted inflammation, because in patients with high AAC index, most of cells, including also the inflammatory ones, are depleted and replaced by bone-like formation, resulting in a very low inflammatory infiltrate. Indeed, the higher levels of inflammation and matrix remodeling are found in patients with medium calcification index.

Inflammatory cell recruitment in AAA is sustained by the presence of inflammatory mediators and by the increased expression of adhesion molecules able to interact with circulating inflammatory cells. [27] Specifically, inflammatory cells infiltrate in the media and adventitia layers, inducing oxidative stress and over expression of cytokines/chemokines and MMPs. The findings obtained by proteomic analyses unveil also the involvement of oxidative stress in AAA patients, underlined by the over expression of the proteins implied in oxidation-reduction process and in cell response to oxidative stress. All these processes lead to elastic fiber breakdown, and depletion of vSMCs. As a result, the aortic wall is weakened because of decreased thickness and reduced mechanical function. The aortic wall cannot counteract the blood flow and pressure, and the aortic wall dilates to form AAA. Among the inflammatory mediators, TNF-α plays a pivotal role in the initiation and progression of vascular disorder by modulating the expression of molecules involved in vascular tone, inflammation and remodeling, thus inducing endothelial dysfunction [28,29] and upregulating the adhesion molecules, such as CD62E. An inflammatory condition, which leads to endothelial dysfunction, contributes to the pathogenesis of vascular syndromes by predisposing vessels to plaque rupture and intravascular thrombosis. [30] Due to endothelial dysfunctions, thus, ECs also contribute to AAA progression. [31]

In our study, we have tested two different percentages of substrate deformation on endothelial cell culture: 5% and 10% for 3 days at 1 Hz constant frequency, representing the resting heartbeat, while the substrate deformation of 10% is selected to mimic the dilation of the aortic wall under physiological conditions. [32] Our experimental settings are consistent with clinical findings on healthy individuals and on AAA patients with medium calcification index. (table 2)

The results suggest that 10% stimulation controls inflammation and ROS/RNS production compared to 5% dynamic and static samples; moreover, this experimental condition significantly contrasts TNF-α-mediated inflammatory effects. Thus, these observations highlight the importance of physiological vascular wall stretching as a powerful anti-inflammatory stimulus. Indeed, a downregulation of MMP-9, CD62E, and a decrease of PBMC adhesion in 10% dynamic samples is observed. In TNF-α-stimulated static samples, MMP-9, CD62E and PBMC adhesion increase, demonstrating that these markers are closely related to the chronic inflammation. Overall, our findings indicate the importance of physiological vascular wall stretching as a powerful anti-inflammatory stimulus able to inhibit the pathological progression of AAA.

Table 2. Summary of obtained data.

	Low AAC index	Medium AAC index	High AAC index
calcium deposits	+	++	+++
dilatation (%)	5 < X < 10	≃ 5	X < 5
inflammation	moderate	high	low
ECM remodeling	moderate	high	moderate

Table 2 shows the results obtained on AAA tissue in terms of calcium accumulation, dilatation, inflammation value, and matrix remodeling.

4. Materials and Methods

4.1. Patients and healthy donors' enrollment

Abdominal aortic aneurysm tissues were provided by the Vascular Surgery Unit, Hospital Maggiore, Novara (Italy). AAA tissues were collected from 13 patients (100% male) subjected to open surgical repair (OSR); demographical and clinical data are reported in Table 3. All data and samples were collected from donors correctly informed for the use of excessive pathological material for diagnostic and research purpose according to the local institute's regulation and policies based on Declaration of Helsinki (AVATAR, 1.0 – protocol 208/CE – CE 43/18). Peripheral blood from healthy donors was collected from AVIS Novara in order to isolate PBMC's (AVATAR, 1.0 – protocol 208/CE – CE 43/18).

4.2. AAA patients: calcification modelling and wall dilatation

Calcificated regions are captured after the CAT exam. The amount of calcification was evaluated through a score (aortic aneurysm calcification-AAC- from 0 to 8): AAC 0-1 are considered low calcification index, AAC 2-3-4 are medium index, and AAC 5-6 high index [13]. Geometries of AAAs are reconstructed, and images of the abdominal aorta are obtained from immediately distal to the renal arteries to immediately proximal to the iliac bifurcation during doppler ultrasound examination. Maximum AAA diameter, determined by B-MODE doppler ultrasound, is 72 mm. The values of aneurysm dilatation are obtained using the following formula:

$$\frac{\boldsymbol{Aortic\ neck\ systole - aortic\ neck\ diastole}}{\boldsymbol{aortic\ neck\ diastole}} : \frac{\boldsymbol{aneurysm\ systole - aneurysm\ diastole}}{\boldsymbol{aneurysm\ diastole}} = \mathbf{0.1} : \boldsymbol{x}$$

Differences between systole and diastole of the aortic neck (healthy part) and the aneurysm are normalized with their respective diastole. The proportion is obtained comparing the differences with 10% that is the physiological measured dilatation of the healthy aorta.

Table 3. Demographical and clinical feature of AAA patients.

Patients	Age mean±SD	Gender	DAAA mean±SD	Hypercholesterolemia	Smoking	Hypertension	Ischemic cardiomyopathy
Low AAC	72±4	Male 100%	5.6±1.4	100%	33%	100%	66%
Medium AAC	75±6	Male 100%	5.4±1.3	50%	50%	88%	50%
High AAC	71±12	Male 100%	5.3±0.6	100%	33%	100%	66%

Table 3 shows demographical data (age, sex) and cardiovascular risk (DAAA aneurysm diameters, hypercholesterolemia, smoking, hypertension, and ischemic cardiomyopathy). Age and DAAA are represented as mean ± standard deviation. Patient data are divided by the grade of aortic calcification index (AAC).

4.3. Histological analyses on human aortic samples

AAA and control samples were fixed in neutral buffered formalin for 24 hours, and 5 μm-thick sections were cut from paraffin-embedded tissues. Briefly, rehydrated sections were treated with a 1% aqueous silver nitrate solution (Sigma Aldrich, Italy). Silver is deposited replacing the calcium reduced by the strong light, and thereby visualized as metallic silver. To counterstain the samples was also used a 5% sodium thiosulfate solution and 0.1% nuclear fast red solution. Calcium deposits and salts are detectable in black or brown-black, nuclei in red and cytoplasm in pink. All images were acquired using Pannoramic MIDI 3DHISTECH and analyzed with Pannoramic Viewer software (3DHISTECH, Hungary). For objective quantification of calcium content ImageJ software was used.

4.4. Proteomic analysis

Tissues obtained from AAA vessel and from healthy control vessel were lysed in RIPA buffer (150 mM sodium chloride, 1% Triton X100, 0.5% sodium deoxycholate, 0.1% sodium dodecyl sulfate, 1 mM EDTA, 1 mM EGTA, 50 mM TRIS pH = 7.4) supplemented with protease inhibitors (0.2 mM sodium othovanadate, 1 mM phenylmethyl sulfonyl fluoride and protease inhibitors cocktail, all from Sigma, Italy). Proteins concentration was determined using the bicinchoninic acid assay (Pierce, Rockford, IL, USA). Lysate proteins were digested using the following protocol: samples were subjected to denaturation with TFE, to reduction with DTT 200 mM, alkylation with IAM 200 mM and the complete protein trypsin digestion with 2 μg of Trypsin/Lys-C (Promega, Madison, WI, USA). The peptide digests were desalted on the Discovery® DSC-18 solid phase extraction (SPE) 96-well Plate (25 mg/well) (Sigma-Aldrich Inc., St. Louis, MO, USA). Peptides were dried by Speed Vacuum until the analysis.

LC–MS/MS analyses were performed on digests using a micro-LC Eksigent Technologies (Dublin, USA) system with a stationary phase of a Halo Fused C18 column (0.5 × 100 mm, 2.7 μm; Eksigent Technologies, Dublin, USA). The injection volume was 4.0 μL and the oven temperature was set at 40 °C. The mobile phase was a mixture of 0.1% (v/v) formic acid in water (A) and 0.1% (v/v) formic acid in acetonitrile (B), eluting at a flow-rate of 15.0 μL min− 1 at an increasing concentration of solvent B from 2% to 40% in 30 min. LC system was interfaced with a 5600 + TripleTOF system (AB Sciex, Concord, Canada) equipped with a DuoSpray Ion Source and CDS (Calibrant Delivery System). The relative abundance of proteins was obtained using the label-free quantification. Samples were subjected to data-dependent acquisition (DDA): the mass spectrometer analysis was performed using a mass range of 100–1500 Da (TOF scan with an accumulation time of 0.25 s), followed by a MS/MS product ion scan from 200 to 1250 Da (accumulation time of 5.0 ms) with the abundance threshold set at 30 cps (35 candidate ions can be monitored during every cycle). The samples were, then, subjected to cyclic data independent analysis (DIA) of the mass spectra, using a 25-Da window: the mass spectrometer was operated such that a 50-ms survey scan (TOF-MS)

was performed and subsequent MS/MS experiments were performed on all precursors.20,21 The MS data were acquired with Analyst TF 1.7 (AB SCIEX, Concord, Canada). Three instrumental replicates for each sample were subjected to the DIA analysis.

Protein identification was performed using Mascot v. 2.4 (Matrix Science Inc., Boston, USA), the digestion enzyme selected was trypsin, with 2 missed cleavages and a search tolerance of 50 ppm was specified for the peptide mass tolerance, and 0.1 Da for the MS/MS tolerance. The charges of the peptides to search for were set to 2 +, 3 + and 4 +, and the search was set on monoisotopic mass. The instrument was set to ESI-QUAD-TOF and the following modifications were specified for the search: carbamidomethyl cysteines as fixed modification and oxidized methionine as variable modification. The UniProt Swiss-Prot reviewed database containing human proteins (version 2015.07.07, containing 42131 sequence entries) was used and a target-decoy database search was performed. False Discovery Rate was fixed at 1%. The label-free quantification was carried out with PeakView 2.0 and MarkerView 1.2. (ABSCIEX, Concord, Canada). The up-regulated proteins were selected using P value < 0.05 and fold change >1.5. The up-regulated proteins were analyzed by using STRING software (http://string-db.org), which is a database of known and predicted protein-protein interactions.

4.5. Dynamic cell culture

Human endothelial cells, EA.hy926 (ATCC® CRL-2922™) were cultured in high-glucose Dulbecco's modified Eagle's medium (DMEM) enriched with 10% fetal bovine serum and penicillin (100 U/mL), streptomycin (100 μg/mL), and 2 mM glutamine mixture (all from Euroclone, Italy) at 37°C in humid 5% CO2 atmosphere. Rectangular silicone pieces (3cm x 1.5cm) were cut and sterilized together with the culture chambers of the TC-3 bioreactor (Ebers Medical, Zaragoza, Spain). To facilitate cell adhesion to the silicone substrate (both static controls and dynamic samples) a type I collagen (50 μg/ml) coating was used. After 1 hour, the coating has been rinsed with sterile water to remove the exceeding collagen. Finally, Ea.hy926 ($2*10^4$ /cm^2) were seeded, and after 24 hours (required for an optimal adhesion to the substrate), mechanical stimulation has been applied to the cell culture. A stretching of 5 and 10% was maintained for 72 hours, 50ng/mL of TNF-α (Sigma Aldrich, Italy) was added when required. Silicone controls were maintained under static conditions.

4.6. Phalloidin staining

Cells were fixed in formalin 4% and incubated with phalloidin TRITC (Sigma Aldrich, Italy) for 45' at 37°C. DAPI (Sigma Aldrich, Italy) was used for nuclear staining. Samples were observed at fluorescent microscope (DM2500 Leica, Germany).

4.7. Cellular ROS/Superoxide Detection Assay kit

Oxidative stress production was investigated through Cellular ROS/Superoxide detection assay kit (ab139476, Abcam, Italy) following the manufacturer's protocol. Briefly, detached cells (static controls, 5%, and 10% of mechanical stimulation) were stained with oxidative stress reagent orange and green, then flow cytometry analyses were performed (ATTUNE NxT Cytometer, Invitrogen) and analysed by ATTUNE NxT flow cytometer software. Pyocyanin treated cells (400μM) were used as positive control.

4.8. Immunofluorescence

Immunofluorescence analyses were carried out on mechanically stimulated silicone cells and on static controls. $1*10^4$ EA.hy926/cm^2 were seeded and maintained in culture according to experimental protocols. After 3 days of stimulation, samples were fixed for 1 hour with 4% formalin. Samples were blocked for 1 hour with a 5% goat solution and 0.3% TRITON X-100 in PBS 1X and, then, incubated with the primary antibody (1:50 anti-E-selectin, Santa Cruz Biotechnology, USA) for 1 hour at room temperature. E-selectin is detected by a secondary antibody TRITC-conjugated (Perkin-Elmer, Italy) and observed at fluorescent microscope (DM2500 Leica, Germany). The images were acquired using

LAS software (Leica, Germany). Data are expressed as TNF-alpha-treated versus the respective untreated samples ratio.

4.9. Leukocyte-endothelium adhesion assay

Peripheral blood mononuclear cells (PBMCs) were isolated with Histopaque®-1077 (Sigma Aldrich, Italy) from peripheral blood obtained by healthy donors. PBMCs adhesion assay was performed using Cell Biolabs' CytoSelectTM Leukocyte-endothelium Adhesion Assay (Cell Biolabs Inc, USA). After mechanical stimulations, PBMCs were labeled by the LeukoTrackerTM solution. Labeled PBMCs were then incubated with static and dynamic cells in presence or not of TNF-α (50ng/mL). After 1 h of incubation, nonadherent cells were removed by gently rinsing with PBS. Adherent cells were counted in three separate fields using an inverted fluorescence microscope (DM2500 Leica, Germany). Data are expressed as TNF-alpha-treated versus the respective untreated samples ratio.

4.10. Western Blot

Culture cells and tissues were lysed in RIPA buffer supplemented with protease inhibitors. Proteins concentration was determined using the bicinchoninic acid assay (Pierce, Rockford, IL, USA). 50µg total proteins in sample buffer (62.5 mM Tris-HCl, pH 6.8, 20% glycerol, 5% β-mercaptoethanol, 0.5% bromophenol blue) were resolved to SDS-PAGE and transferred to a nitrocellulose membrane (Amersham Biosciences, Buckinghamshire, UK). Membranes were incubated overnight with IL-6, OPN (Abcam, UK), MMP-9, Tubulin (Millipore, Italy) antibodies at 4°C. Proteins were revelated with secondary antibody-peroxidase conjugates (Perkin-Elmer, Italy). Protein bands were visualized using ECL (Perkin-Elmer, Western lightning PLUS-ECL, Italy) detection reagents in a chemosensitive visualizer (VersaDoc, BioRad, Italy). In order to check the loaded proteins concentration, red ponceau (Sigma Aldrich, Italy) staining was considered.

4.11. Zymography assay

Non-reduced protein samples were resolved by SDS-PAGE gels containing gelatin (0.2%, Sigma Aldrich, Italy). Briefly, after electrophoresis, gels were incubated with TRITON X-100 for 3 h at room temperature, and then incubated in a solution of CaCl2 (1 mM) and NaCl (15 mM), pH 7.4 overnight at 37°C. Subsequently, gels were fixed and then stained with Coomassie Blue. For objective quantification ImageJ software was used.

4.12. Statistical analyses

All experiments were performed in triplicate. All data are expressed as mean values ± standard deviation. Using Student's t-test, the p-value is calculated and the differences between variables with a value of $p < 0.05$ are considered statistically significant.

5. Conclusions

In conclusion, we found a negative correlation between calcium deposits and wall dilatation in presence of AAA. A decreased wall stretching, due to the presence of calcification, affects MMP-9-mediated matrix degradation and IL-6-mediated inflammation. As expected, *in vitro* model on endothelial cell line shows that substrate deformation significantly regulates the inflammatory response and matrix remodeling.

Author Contributions: Conceptualization: M.R., G.B., M.T., M.M., F.B.; Methodology: M.R., G.B., M.M., M.T., F.C., Validation: F.B., L.G.F.; Investigation, M.R., G.B., M.T., L.F., M.M., M.C., F.C., F.B.; Data Curation, M.R., G.B., M.T., F.C.; Writing – Original Draft Preparation: M.R., G.B.; Writing – Review & Editing: L.F., M.T., M.M., M.C., C.P., R.B., L.G.F., E.M., F.B.; Supervision: C.P., R.B., L.G.F., E.M., F.B.; Project Administration: R.B., L.G.F., F.B.; Funding Acquisition: R.B., L.G.F., E.M., F.B.

Funding: Part of this research was funded by TissueGraft s.r.l.

Acknowledgments: The authors would like to thank Dr. Carlino and Prof. Mascaro from AVIS Novara for blood collection.

Conflicts of Interest: The authors declare no conflict of interest

Abbreviations

AAA	Abdominal Aortic Aneurysm
ECs	Endothelial cells
TNF-α	Tumor necrosis factor alpha
MMP-9	Matrix metalloproteinase -9
ECM	Extracellular matrix
PTM	transmural pressure
vSMCs	Vascular smooth muscle cells
IL-1	Interleukin-1
IL-6	Interleukin-6
IL-8	Interleukin-8
MCP-1	Monocyte chemoattractant protein 1
RANTES	Regulated on activation, normal T cell expressed and secreted
CAMs	Cell adhesion molecules
ROS	Reactive oxygen species
NADPH	Nicotinamide adenine dinucleotide phosphate
NOX	Nicotinamide adenine dinucleotide phosphate oxidase
XO	Xanthine oxidase
SOD	Superoxide dismutase
TRX	Thioredoxin
MMPs	Matrix metalloproteinases
NF-kB	Nuclear factor kappa-light-chain-enhancer of activated B cells
AP-1	Activator protein 1
OPN	Osteopontin
CAT	Computed axial tomography
AAC	Aortic aneurysm calcification
RNS	Reactive nitrogen species
APOE	Apoliprotein E
OSR	Open surgical repair
DAAA	Diameter of abdominal aortic aneurysm
TFE	Trifluoroethanol
DTT	Dithiothreitol
IAM	Iodoacetamide
LC-MS/MS	Liquid chromatography– tandem mass spectrometry
CDS	Calibrant Delivery System
DDA	Data-dependent acquisition
TOF	Time of flight
DIA	Data independent analysis
DMEM	Dulbecco's modified Eagle's medium
TRITC	Tetramethylrhodamine
DAPI	4′,6-Diamidine-2′-phenylindole dihydrochloride
RIPA	Radioimmunoprecipitation buffer
EDTA	Ethylenediamenetetraacetic acid
EGTA	Ethyleneglycol-bis(2-aminoethylether)-N,N,N',N'-tetraacetic acid
SDS-PAGE	Sodium dodecyl sulfate polyacrylamide gel electrophoresis
PBMCs	Peripheral blood mononuclear cells
PBS	Phosphate Buffered Saline
PBMCs	Peripheral blood mononuclear cells

References

1. Moxon, J. V.; Parr, A.; Emeto, T.I.; Walker, P.; Norman, P.E.; Golledge, J. Diagnosis and Monitoring of Abdominal Aortic Aneurysm: Current Status and Future Prospects. *Curr. Probl. Cardiol.* **2010**, 35, 512–548, doi:10.1016/j.cpcardiol.2010.08.004.
2. Forsdahl, S.H.; Singh, K.; Solberg, S.; Jacobsen, B.K. Risk factors for abdominal aortic aneurysms: a 7-year prospective study: the tromsø study, 1994 2001. *Circulation* **2009**, 119, 2202–2208, doi:10.1161/CIRCULATIONAHA.108.817619.
3. Vardulaki, K.A.; Prevost, T.C.; Walker, N.M.; Day, N.E.; Wilmink, A.B.M.; Quick, C.R.G.; Ashton, H.A.; Scott, R.A.P. Incidence among men of asymptomatic abdominal aortic aneurysms: Estimates from 500 screen detected cases. *J. Med. Screen.* **1999**, 6, 50–54, doi:10.1136/jms.6.1.50.
4. Lederle, F.A.; Johnson, G.R.; Wilson, S.E.; Littooy, F.N.; Krupski, W.C.; Bandyk, D.; Acher, C.W.; Chute, E.P.; Hye, R.J.; Gordon, I.L.; et al. Yield of repeated screening for abdominal aortic aneurysm after a 4-year interval. *Arch. Intern. Med.* **2000**, 160, 1117–1121, doi:10.1001/archinte.160.8.1117.
5. Scott, R.A.P.; Ashton, H.A.; Buxton, M.J.; Day, N.E.; Kim, L.G.; Marteau, T.M.; Thompson, S.G.; Walker, N.M. The Multicentre Aneurysm Screening Study (MASS) into the effect of abdominal aortic aneurysm screening on mortality in men: A randomised controlled trial. *Lancet* **2002**, 360, 1531–1539, doi:10.1016/S0140-6736(02)11522-4.
6. Lindholt, J.S.; Juul, S.; Fasting, H.; Henneberg, E.W. Screening for abdominal aortic aneurysms: Single centre randomised controlled trial. *Br. Med. J.* **2005**, 330, 750–752, doi:10.1136/bmj.38369.620162.82.
7. Ashton, H.A.; Gao, L.; Kim, L.G.; Druce, P.S.; Thompson, S.G.; Scott, R.A.P. Fifteen-year follow-up of a randomized clinical trial of ultrasonographic screening for abdominal aortic aneurysms. *Br. J. Surg.* **2007**, 94, 696–701, doi:10.1002/bjs.5780.
8. Nordon, I.M.; Hinchliffe, R.J.; Loftus, I.M.; Thompson, M.M. Pathophysiology and epidemiology of abdominal aortic aneurysms. *Nat. Rev. Cardiol*. **2011**, 8, 92–102, doi:10.1038/nrcardio.2010.180.
9. Rodella, L.F.; Rezzani, R.; Bonomini, F.; Peroni, M.; Cocchi, M.A.; Hirtler, L.; Bonardelli, S. Abdominal aortic aneurysm and histological, clinical, radiological correlation. *Acta Histochem*. **2016**, 118, 256–262, doi:10.1016/j.acthis.2016.01.007.
10. Emeto, T.I.; Moxon, J. V; Biros, E.; Rush, C.M.; Clancy, P.; Woodward, L.; Moran, C.S.; Jose, R.J.; Nguyen, T.; Walker, P.J.; et al. Urocortin 2 is associated with abdominal aortic aneurysm and mediates anti-proliferative effects on vascular smooth muscle cells via corticotrophin releasing factor receptor 2. *Clin Sci* **2013**, doi:10.1042/CS20130425.
11. Wassef, M.; Baxter, B.T.; Chisholm, R.L.; Dalman, R.L.; Fillinger, M.F.; Heinecke, J.; Humphrey, J.D.; Kuivaniemi, H.; Parks, W.C.; Pearce, W.H.; et al. Pathogenesis of abdominal aortic aneurysms: A multidisciplinary research program supported by the National Heart, Lung, and Blood Institute. *J. Vasc. Surg*. **2001**, 34, 730–738, doi:10.1067/mva.2001.116966.
12. Buijs, R.V.C.; Willems, T.P.; Tio, R.A.; Boersma, H.H.; Tielliu, I.F.J.; Slart, R.H.J.A.; Zeebregts, C.J. Calcification as a risk factor for rupture of abdominal aortic aneurysm. *Eur. J. Vasc. Endovasc. Surg*. **2013**, 46, 542–548, doi:10.1016/j.ejvs.2013.09.006.
13. Lederle, F.A.; Johnson, G.R.; Wilson, S.E.; Gordon, I.L.; Chute, E.P.; Littooy, F.N.; Krupski, W.C.; Bandyk, D.; Barone, G.W.; Graham, L.M.; et al. Relationship of age, gender, race, and body size to infrarenal aortic diameter. *J. Vasc. Surg.* **1997**, 26, 595–601, doi:10.1016/S0741-5214(97)70057-0.
14. Chiu, J.-J.; Chien, S. Effects of dsisturbed flow on vascular endothelium: pathophysiological basis and clinical perspectives. *Physiol Rev* **2011**, 91, 327–387, doi:10.1152/physrev.00047.2009.
15. Davies, P.F. Flow-Mediated Endothelial Mechanotransduction. *NIH Public Access* **1995**, 75, 519–560, doi:10.1016/j.drudis.2011.09.009.
16. KOFLER, S.; NICKEL, T.; WEIS, M. Role of cytokines in cardiovascular diseases: a focus on endothelial responses to inflammation. *Clin. Sci.* **2005**, 108, 205–213, doi:10.1042/CS20040174.
17. Mackay, C.R. Chemokines: Immunology's high impact factors. *Nat. Immunol*. **2001**, 2, 95–101, doi:10.1038/84298.
18. Golias, C.H.; Tsoutsi, E.; Matziridis, A.; Makridis, P.; Batistatou, A.; Charalabopoulos, K. Leukocyte and endothelial cell adhesion molecules in inflammation focusing on inflammatory heart disease. *In Vivo* (Brooklyn). **2007**, 21, 757–770.
19. Tsutsui, H.; Kinugawa, S.; Matsushima, S. Oxidative stress and heart failure. *Am. J. Physiol. Heart Circ. Physiol*. **2011**, 301, H2181-90, doi:10.1152/ajpheart.00554.2011.

20. McCormick, M.L.; Gavrila, D.; Weintraub, N.L. Role of oxidative stress in the pathogenesis of abdominal aortic aneurysms. *Arter. Thromb Vasc Biol* **2007**, 27, 461–469, doi:10.1161/01.ATV.0000257552.94483.14.
21. Forstermann, U. Oxidative stress in vascular disease: causes, defense mechanisms and potential therapies. *Nat Clin Pr. Cardiovasc Med* **2008**, 5, 338–349, doi:10.1038/ncpcardio1211.
22. Forstermann, U. Nitric oxide and oxidative stress in vascular disease. *Pflugers Arch* **2010**, 459, 923–939, doi:10.1007/s00424-010-0808-2.
23. Parodi, F.E.; Mao, D.; Ennis, T.L.; Bartoli, M.A.; Thompson, R.W. Suppression of experimental abdominal aortic aneurysms in mice by treatment with pyrrolidine dithiocarbamate, an antioxidant inhibitor of nuclear factor-κB. *J. Vasc. Surg*. **2005**, 41, 479–489, doi:10.1016/j.jvs.2004.12.030.
24. Costanzo, A.; Moretti, F.; Burgio, V.L.; Bravi, C.; Guido, F.; Levrero, M.; Puri, P.L. Endothelial activation by angiotensin II through NFκB and p38 pathways: Involvement of NFκB-inducible kinase (NIK), free oxygen radicals, and selective inhibition by aspirin. *J. Cell. Physiol*. **2003**, 195, 402–410, doi:10.1002/jcp.10191.
25. Li, Q.; Engelhardt, J.F. Interleukin-1beta induction of NFkappaB is partially regulated by H2O2-mediated activation of NFkappaB-inducing kinase. *J Biol Chem* **2006**, 281, 1495–1505, doi:M511153200 [pii]\r10.1074/jbc.M511153200.
26. Ramella, M.; Bernardi, P.; Fusaro, L.; Manfredi, M.; Casella, F.; Porta, C.M.; Nicolai, L.; Galeazzi, E.; Boldorini, R.; Settembrini, A,M.; Settembrini, P.; Marengo, E.; Cannas, M.; Boccafoschi, F. Relevance of inflammation and matrix remodeling in abdominal aortic aneurysm (AAA) and popliteal artery aneurysm (PAA) progression. *Am J Transl Res* **2018**, 10(10), 3265-3275.
27. Wang, Q.; Ren, J.; Morgan, S.; Liu, Z.; Dou, C.; Liu, B. Monocyte Chemoattractant Protein-1 (MCP-1) regulates macrophage cytotoxicity in abdominal aortic aneurysm. *PLoS One* **2014**, 9, doi:10.1371/journal.pone.0092053.
28. Palmieri, D.; Perego, P.; Palombo, D. Estrogen receptor activation protects against TNF-α-induced endothelial dysfunction. *Angiology* **2014**, 65, 17–21, doi:10.1177/0003319713477909.
29. Zhang, H.; Park, Y.; Wu, J.; Chen, X.; Lee, S.; Yang, J.; Dellsperger, K.C.; Zhang, C. Role of TNF-alpha in vascular dysfunction. *Clin Sci* **2009**, 116, 219–230, doi:CS20080196 [pii]\r10.1042/CS20080196.
30. Hadi, H.A.R.; Carr, C.S.; Al Suwaidi, J. Endothelial Dysfunction: Cardiovascular Risk Factors, Therapy, and Outcom. *Vasc Health Risk Manag* **2005**, 1(3), 183–198.
31. Ramella, M.; Boccafoschi, F.; Bellofatto, K.; Follenzi, A.; Fusaro, L.; Boldorini, R.; Casella, F.; Porta, C.; Settembrini, P.; Cannas, M. Endothelial MMP-9 drives the inflammatory response in abdominal aortic aneurysm (AAA). *Am. J. Transl. Res*. **2017**, 9(12), 5485-5495.
32. Golledge, J.; Muller, J.; Daugherty, A.; Norman, P. Abdominal aortic aneurysm: Pathogenesis and implications for management. *Arterioscler. Thromb. Vasc. Biol.* **2006**, 26, 2605–2613.